Photonic Neural Networks without Nonlinear Optical Devices

Kojima, Keisuke; Koike-Akino, Toshiaki

TR2026-102 July 03, 2026

Abstract

We propose to use data reuploading techniques for photonic neural networks to replace nonlinear optical devices with phase modulators. Simulation results indicate similar accuracy and power consumption in both cases, offering an alternative implementation option.

Conference on Lasers and Electro-Optics (CLEO) 2026

Photonic Neural Networks without Nonlinear Optical Devices

Keisuke Kojima[1,*] and Toshiaki Koike-Akino[2]

[1] *Boston Quantum Photonics LLC, 588 Boston Post Rd #315, Weston, MA 02493, USA*
[2] *Mitsubishi Electric Research Laboratories (MERL), 201 Broadway, Cambridge, MA 02139, USA*

[*] *kkojima@bostonqp.com*

Abstract: We propose to use data reuploading techniques for photonic neural networks to replace nonlinear optical devices with phase modulators. Simulation results indicate similar accuracy and power consumption in both cases, offering an alternative implementation option.

1. Introduction

Photonic neural networks (PNNs) [1] are expected to play a major role in the future data processing area, where high speed and low power consumptions are required. Multiple architectures are proposed. However, most architectures require nonlinear optical devices (NLODs) to simulate the activation functions. Although there are many proposals and experimental verifications for achieving optical nonlinearities [2], in reality, considering the cascadabilities and robustness, hybrid photonic-electronic implementation is most practical [1,3]; however, this requires high speed photo diodes (PDs), electronic nonlinear devices/amplifiers, and high speed modulators.

The data reuploading (DR) technique [4], originally introduced in the context of quantum computing to achieve universal approximation, provides an alternative pathway. We previously applied data reuploading to realize universal non-quantum photonic computing using standard photonic integrated circuits (PICs) [5]. Follow-up work explored more robust and scalable implementations [6], and polarization-domain encoding [7]. These earlier configurations relied on relatively long cascades of photonic elements to repeatedly reintroduce the input data.

In this work, we show that DR can be integrated directly into the conventional Clements interferometer mesh [8]. This enables the mesh to realize nonlinear decision boundaries without any NLODs or hybrid O/E/O activation stages, and without sacrificing inference accuracy. The proposed formulation preserves the compact, unitary, and fabrication-friendly nature of the Clements architecture while providing a practical route to scalable, all-passive photonic neural networks.

2. Network Configurations

Fig. 1(a) presents a conventional PNN model using NLODs. The network implements arbitrary real-valued matrices via singular value decomposition ($U\Sigma V$). Unitary operators U and V are realized using Clements-type rectangular meshes of Mach–Zehnder interferometers (MZIs) with phase shifters (PSs). The diagonal matrix Σ is an array of MZIs configured as attenuators. Input data are encoded by amplitude modulators (AMs), which can also be MZI-based.

The optical nonlinearity is modeled in three steps: a photodetector (PD) measures the signal intensity ($I = |x|^2$); an electronic square-root function processes the signal; and a high-speed intensity modulator re-encodes the result

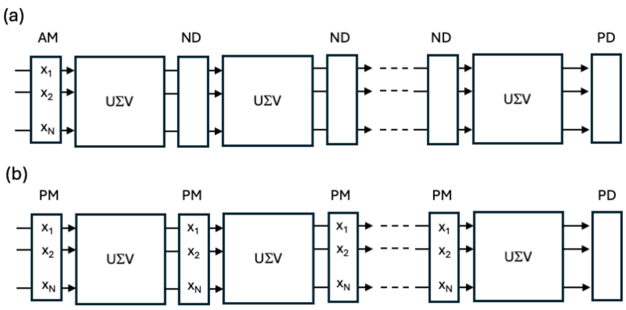

Fig. 1: (a) Comparison of PNN configurations: (a) conventional PNN utilizing nonlinear optical devices (NLOD), and (b) the proposed PNN implementing data reuploading with repeated phase modulation (PM). AM: Amplitude Modulator, PD: Photodetector.

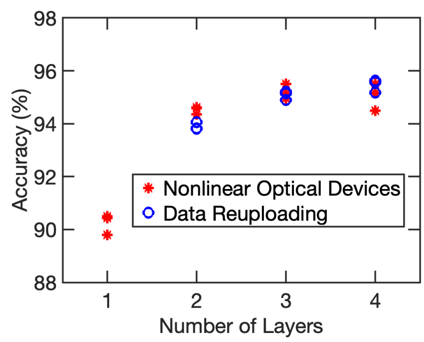

Fig. 2: Accuracy of PNNs versus the number of layers for NLOD and DR implementations. The 1-layer case indicates the baseline Clements-mesh without NLODs.

optically. The final optical outputs, detected by a PD array, are interpreted as class scores.

Fig.1(b) shows a DR-based PNN model with an architecture similar to Fig.1(a). The major difference is that input data are repeatedly applied via phase modulators (PMs). If optical loss is sufficiently low, this configuration achieves a purely passive optical neural network. While this approach requires high-speed PMs such asthin-film lithium niobate (TFLN), barium titanate (BTO), or Si-based, this drawback is offset because the conventional setup in Fig. 1(a) similarly requires high-speed AMs for its NLODs.

3. Simulations

Simulations are conducted using the PyTorch library. We use the MNIST dataset for evaluation, which consist of 64,000 training and 10,000 test images, each 28×28 pixels. The task is a 10-class classification problem, so the labels are represented as one-hot vectors of length 10.

To simulate linear optical compression of high-dimensional fields, we first employ a linear autoencoder to reduce the 784-dimensional image vectors to an 18-dimensional representation. These 18 features serve as inputs to the PNN under test. with cross-entropy loss used as the training objective.

Test accuracy versus the number of layers is shown in Fig. 2. Results from three independent training runs are plotted as individual points for each condition. The plot demonstrates comparable classification performance between the conventional NLOD approach and the proposed data-reuploading method using only phase modulators.

4. Power Consumption Analysis

Both PNN architectures share many common components. We assume each PS requires 20 mW for a π shift and has an average operating power of 10 mW. For one $U\Sigma V$ layer, which include the attenuation stage, the number of PSs is $342(18 \times 17 + 2 \times 18)$ PSs, resulting in a total PS power consumption of approximately 3.42 W per layer. For the optical source, We assume 0.1 W of electrical power generates 30 mW of optical power, which is then split across the 18 input channels. Finally, the transimpedance amplifiers (TIAs) associated with the PDs are each assumed to consume 100 mW.

For the conventional PNN configuration, AMs are implemented using silicon MZMs. We assume a power consumption of 40 mW for the CMOS driver and 20 mW for the MZM at 10 Gb/s. The nonlinear optical activation stage, which includes detecting optical power with PDs and TIAs, amplifying the signal, exploiting the nonlinear portion of the modulator's transfer function—together, and an additional laser source, consumes approximately 100 mW, 40 mW, and 20 mW, respectively, in addition to the common laser source of 100 mW. Total power is 12.4 W for 2 layers and 24.7 W for 4 layers, equivalent to 1.24 pJ and 2.47 pJ per operation, respectively.

The data uploading configuration uses a TFLN modulator and driver (combined 92 mW at 10 Gbps). A semiconductor optical amplifier (SOA) is assumed after the second layer, consuming 100 mW each. The SOA requirement will depend on the mesh passive losses, laser power, and modulation speed. The total power is 11.7 W and 23.3 W with 2 and 4 layers, equivalent to 1.17 pJ and 2.33 pJ per operation, respectively.

For the electronic counterpart of this operation, we assume a three layer neural network with 18, 32, and 10 dimensions using ReLU as the activation function. This configuration achieves 95.6% accuracy on the same dataset. The network requires $18 \times 32 + 32 \times 10 = 896$ multiply-accumulate (MAC) operations, and this is equivalent to 0.9 nJ per operation, where state-of-the art electronic components consumes about 1 pJ/MAC.

Overall, the power consumption of conventional and DR PNNs are comparable for the same number of layers, and are 2 to 3 orders of magnitude smaller than their electronic counterpart.

5. Conclusion

We established the Clements-mesh PNN as a baseline for comparison against conventional NLOD and DR cases. The DR approach yields comparable simulated accuracy and power consumption to conventional PNNs, suggesting DR as a viable option for practical implementations.

References

1. , Y. Shen, N. C. Harris, S. Skirlo, M. Prabhu, T. Baehr-Jones, M. Hochberg, X. Sun, S. Zhao, H. Larochelle, D. Englund *et al.*, Nat. photonics **11**, 441–446 (2017).
2. , N. Takahashi, W. Fang, R. Xue, S. Okada, Y. Ohiso, T. Amemiya, and N. Nishiyama, Opt. Lett. **47**, 5715–5718 (2022).
3. , I. A. Williamson, T. W. Hughes, M. Minkov, B. Bartlett, S. Pai, and S. Fan, IEEE J. Sel. Top. Quantum Electron. **26**, 1–12 (2019).
4. , A. Pérez-Salinas, A. Cervera-Lierta, E. Gil-Fuster, and J. I. Latorre, Quantum **4**, 226 (2020).
5. K. Kojima and T. Koike-Akinoin *SPIE Photonics for Quantum,* (SPIE, 2024).
6. T. Koike-Akino, K. Kojima, and M. Taguchiin *AI and Optical Data Sciences VI,* vol. 13375 (SPIE, 2025), pp. 117–124.
7. M. Taguchi, T. Koike-Akino, A. Hosaka, T. Yoshida, and K. Kojimain *IEEE Photonics Conference,* (IEEE, 2025), p. P33.
8. , W. R. Clements, P. C. Humphreys, B. J. Metcalf, W. S. Kolthammer, and I. A. Walmsley, Optica **3**, 1460–1465 (2016).